Pharmacokinetics and Pharmacodynamics of 7-Nitroindazole, a Selective Nitric Oxide Synthase Inhibitor, in the Rat Hippocampus

Mark A. Bush[1,2] and Gary M. Pollack[1,3]

Received July 23, 2001; accepted July 30, 2001

Purpose. This study was conducted to assess the pharmacokinetics and pharmacodynamics of 7-nitroindazole (7-NI), a selective inhibitor of neuronal nitric oxide synthase (NOS).

Methods. Male Sprague-Dawley rats were equipped with peritoneal/venous cannulae and a microdialysis probe in the hippocampal cortex. Rats received 7-NI in peanut oil (25 mg/kg) ip every 2 h for 14 h or peanut oil alone. Blood samples were obtained at timed intervals for serum 7-NI; brain tissue microdialysate for determination of extracellular 7-NI and NO was obtained every 20 min. A pharmacokinetic-pharmacodynamic model was constructed to evaluate the effects of 7-NI on NOS activity.

Results. Consistent with previous reports, NOS activity in controls evidenced circadian variation. These cyclic changes in NO production were incorporated into the model of 7-NI effects on NOS. 7-NI produced a rapid (within 2 h) decrease in hippocampal NO. Under the conditions of this experiment, 7-NI produced an ~50% decrease in hippocampal NO, which was sustained during 7-NI administration. The decrease in NOS activity by 7-NI was concentration-dependent with an apparent IC_{50} of ~17 μg/ml.

Conclusions. Multiple ip injections of 7-NI result in a predictable, sustained decrease in NO production in the hippocampus. The pharmacokinetic-pharmacodynamic model developed allows design of dosing regimens that can produce designated changes in brain NO content, facilitating use of 7-NI to probe the pharmacological implications of NO in the central nervous system.

KEY WORDS: 7-nitroindazole; nitric oxide synthase; microdialysis; pharmacodynamics.

INTRODUCTION

Nitric oxide (NO) has been shown to be involved in multiple processes in the central nervous system such as long-term potentiation (1), seizure activity (2), memory (3), nociceptive processing (4), and development of tolerance to centrally acting compounds such as opioids (5) and ethanol (6). An important method for the determination of the roles of NO in the central nervous system (CNS) is the use of inhibitors of nitric oxide synthase (NOS). Whereas specific inhibitors (i.e., that interact with only a single isoform) of neuronal NOS (type I) are unavailable, inhibitors that are selective for type I NOS (i.e., preferentially inhibit type I, but may interact to a limited extent with other isoforms) have been identified (7). The heterocyclic compound 7-nitroindazole (7-NI), which inhibits NOS by competing with both L-arginine and tetrahydrobiopterin (8), has been used extensively as a selective inhibitor of neuronal NOS (9–11). 7-NI evidences a 10-fold selectivity for neuronal NOS (8).

Relative selectivity for type I NOS inhibition is advantageous when evaluating the role of NOS in the CNS. Non-selective inhibitors of NOS (e.g., N^{ω}-nitro-L-arginine) are capable of significantly reducing endothelial and inducible NOS activity in addition to inhibition of neuronal NOS. One consequence of such generalized inhibition is an elevation of systemic blood pressure (12) resulting in reduced sensitivity to nociceptive stimuli (13). As a result, inhibitors of NOS that produce significant hypertensive responses have limited use in elucidating the role of NO in nociceptive processing. An advantage to the use of 7-NI in evaluation of antinociceptive tolerance is the reported lack of effect of this NOS inhibitor on systemic blood pressure (14,15).

Research into the roles of NO in biological processes is still at a relatively early stage. At present, extensive pharmacokinetic/pharmacodynamic data are available only for the non-selective NOS inhibitor N^{ω}-nitro-L-arginine (16–18). As a consequence, use of NOS inhibitors to probe the physiological functions of NO has depended on empirical dosing regimens. Previous studies in this laboratory (19) were performed to evaluate the systemic pharmacokinetics of 7-NI following a single intraperitoneal injection. These data allowed the design of appropriate dosage regimens to maintain selected concentrations of 7-NI in serum. However, it also is important to understand how NOS activity in the CNS correlates with 7-NI concentrations in serum and brain tissue. Such information is necessary for the design of 7-NI dosing regimens intended to maintain a desired degree of NOS inhibition. The present study was performed to evaluate the relationship between systemic and hippocampal disposition of 7-NI and to evaluate the relevant pharmacodynamic parameters for 7-NI-mediated inhibition of hippocampal NOS through a pharmacokinetic/pharmacodynamic modeling approach.

MATERIALS AND METHODS

Chemicals

7-NI (Sigma, St. Louis, MO) was formulated as a suspension in peanut oil (33.3 mg/ml). All other reagents and solvents were obtained from commercial sources and were of the highest purity available.

Animals

Animal procedures adhered to the *Principles of Laboratory Animal Care* (NIH publication #85–23). Male Sprague-Dawley rats (Hilltop Laboratory Animals Inc., Scottdale, PA), weighing 275 to 350 g, were housed ≥5 days in a temperature-controlled facility (72 ± 2°F, 12-h light/dark cycle). Access to food (LabDiet, PMI Feeds, St. Louis, MO) and water was allowed at all times. Rats were anesthetized with ketamine (50 mg/kg) and xylazine (10 mg/kg) ip and received a prophylactic dose of penicillin G (50,000 U/kg) by intramuscular injection 24 h before the experiment. Surgical sites were shaved and cleaned with Betadine, and silicone rubber can-

[1] Division of Drug Delivery and Disposition, School of Pharmacy, The University of North Carolina at Chapel Hill, Chapel Hill, North Carolina 27599-7360.

[2] Current address: Chiron Corporation, 4560 Horton Street, Emeryville, California 94806.

[3] To whom correspondence should be addressed. (e-mail: gary_pollack@unc.edu)

0724-8741/01/1100-1607$19.50/0

nulae were implanted in the right jugular and right femoral veins. The cannulae were exteriorized in the dorsal neck region, and patency was maintained by flushing with heparinized saline (20 U/ml).

To avoid repeated ip injections, ip cannulae were implanted. Polyethylene (PE60) tubing was heat-bent to approximate the contours of the animal. A cuff was constructed at one end by melting the tip of the cannula. A puncture wound was made through the abdominal wall with a 20-gauge needle, and the cuffed end of the tubing was inserted into the peritoneal space. Musculature was sutured with surgical silk, and a small amount of surgical adhesive was used to secure the tubing. The incision above the site of implantation was sutured with surgical silk and further secured with adhesive. The distal end of the cannula was tunneled subcutaneously and exteriorized at the dorsal neck region.

To implant the microdialysis probe in the hippocampus, rats were placed in a rodent stereotaxic frame (David Kopf Instruments, Tujunga, CA). A midline incision was made in the scalp starting at an interaural position and proceeding ~2-cm rostral. Connective tissue was removed with a cotton swab, and a hole was trephined in the skull (Bregma −5.60, Lateral +5.00, DV −7.00), and a CMA/12 guide cannula (CMA, Acton, MA) was inserted slowly to a depth of 3 mm below the dura. The opening in the skull surrounding the guide cannula was sealed with bone wax, and the cannula was secured with dental acrylic cement (DuraLay, Reliance Dental Manufacturing Co., Worth, IL). A CMA/12 (3 mm) microdialysis probe, previously flushed with distilled deionized water, was inserted slowly into the guide cannula. The inlet and outlet ports of the probe were sealed until the experiment to prevent drying of the probe. Following experimentation, probes were perfused with a 1% solution of trypan blue for 15 min and animals were sacrificed and examined for hippocampal staining to confirm appropriate positioning of the microdialysis probe.

Experimental

Rats were placed in a microdialysis apparatus (CMA, Acton, MA) allowing unrestricted locomotion. Microdialysis probes were equilibrated by perfusing with artificial cerebrospinal fluid (147 mM NaCl, 3.0 mM KCl, 1.0 mM $MgCl_2$, 1.3 mM $CaCl_2$, 1.0 mM NaH_2PO_4) at 5 μl/min, and baseline NO (expressed as the sum of nitrate and nitrite concentrations; NO_x^-) concentrations were determined over a 2-h interval. Rats then received 7-NI (33.3 mg/ml in peanut oil) via the peritoneal cannula as a 50-mg/kg loading dose followed by 25 mg/kg every 2 h for 14 h, or peanut oil alone by the same schedule (n = 4/group). All rats received an infusion of normal saline (2 ml/h via the femoral vein) to maintain hydration for the duration of the experiment. Microdialysate (100 μl) was collected every 20 min, and blood was obtained through the jugular cannula. Serum and microdialysate samples were stored at −20°C pending analysis.

Analysis of 7-NI

A sensitive and specific HPLC assay for determination of 7-NI has been developed (19). Briefly, serum (100 μl) or microdialysate (80 μl) was thawed, and 30 μl of *p*-nitroaniline (PNA; 5 μg/ml in water) was added as an internal standard. Samples were mixed by vortex and adjusted to 230 μl (serum) or 150 μl (microdialysate) with water. For serum, ice-cold acetonitrile (460 μl) was added and samples were mixed by vortex and centrifuged (3,000*g,* 5 min). The supernatant was collected and evaporated to dryness under nitrogen. Evaporated samples were reconstituted in 150 μl of mobile phase with vigorous mixing to ensure dissolution of sample components. Aliquots (50 μl) of sample were injected on-column for analysis. Chromatographic separation was achieved on a BDS-Hypersil C8 column (250 × 4.6 mm, 5 μm) with a mobile phase (pH 4.5; acetonitrile [18%], acetate buffer [82%; 20 mM, pH 4.0], and triethylamine [0.05%]) flow rate of 1 ml/min. Absorbance of eluent was monitored at 360 nm. Under these conditions, PNA and 7-NI eluted at 22 and 26 min, respectively.

Probe Recovery for 7-NI

To estimate concentrations of 7-NI in hippocampal extracellular fluid, it was necessary to evaluate the recovery of 7-NI by each microdialysis probe. *In vitro* recoveries of 7-NI and PNA were not statistically different (35.6 ± 0.2 vs. 35.0 ± 0.4%, respectively) at physiological pH. Therefore, PNA was used to determine the *in vivo* probe efficiency by retrodialysis. At the end of each microdialysis study, a solution of PNA in artificial cerebrospinal fluid (1 μg/ml) was perfused through the microdialysis probe, and the probe effluent was collected and analyzed by HPLC for PNA. The fractional loss of PNA across the probe membrane provided an estimate of probe efficiency (20). Concentrations of 7-NI measured in microdialysate were corrected for probe efficiency to estimate the extracellular fluid concentration *in vivo*.

Analysis of NO_x^- Concentrations

NO has an extremely short half-life *in vivo* and is converted predominately to NO_3^- and NO_2^- (NO_x^-). Due to the relative stability of these products, NOS activity was assessed by quantitating NO_x^- in microdialysate with a modification of the Griess assay (21). Aliquots (80 μl) of microdialysate were transferred to amber-colored polypropylene tubes, and nitrate was converted to nitrite enzymatically. NADPH (10 μl; 1 μM final concentration) was added to each sample with mixing by vortex. A mixture containing glucose-6-phosphate, glucose-6-phosphate dehydrogenase, and nitrate reductase (10 μl; final concentrations 0.5 mM, 160 mU/ml, and 80 mU/ml, respectively) was added with brief mixing and incubation (25°C, 1 h) to convert nitrate to nitrite. Sample temperature was reduced to ~4°C by placing tubes on ice (30 min). Sulfanilamide and HCl (17 μl each; 1 mM and 0.6 mM final concentration, respectively) were added, samples were mixed after each addition, and incubated on ice for 15 min. *N*-(1-naphthyl)-ethylenediamine (17 μl; 1 mM final concentration) was added, and samples were mixed and incubated (25°C, 30 min). Spectrophotometric analysis (absorbance at 548 nm) of samples was performed on a Beckman DU 640 spectrophotometer modified with a Micro Auto-1 accessory cell holder for a microcell (minimum volume 50 μl) cuvette (Beckman Instruments, Fullerton, CA). Standard curve analyses were performed to verify that absorbance of the azo dye formed was linearly related to the NO_x^- concentration.

Pharmacokinetic/Pharmacodynamic Modeling

To evaluate the parameters associated with NOS inhibition by 7-NI, it was necessary to describe the disposition of 7-NI in the hippocampus, time-dependent oscillation of baseline NO_x^- concentrations, and the relationship between NOS activity and 7-NI concentration. Due to the lack of data regarding 7-NI disposition following iv administration, determination of explicit pharmacokinetic parameters for 7-NI was not possible. However, an empirical model was developed to describe 7-NI disposition in the hippocampus following ip administration. Because 7-NI equilibrated rapidly between hippocampal extracellular fluid and serum, and estimated unbound concentrations in serum (19) were equivalent to concentrations in hippocampal extracellular fluid, hippocampal extracellular fluid was indistinguishable from the central pharmacokinetic compartment. Thus, the pharmacokinetic model was comprised of an absorption compartment (peritoneal cavity) and a central compartment (volume = V_c), which contained both serum and hippocampal extracellular fluid. The rate constants for absorption into (k_a) and elimination from (K) the central compartment were assumed to be first order at the 7-NI doses administered in this experiment. Administration of 7-NI into the absorption compartment occurred *via* rapid infusion (k_0).

NO_x^- concentrations in the hippocampus of control rats displayed cyclic fluctuations throughout the experiment. To approximate these fluctuations, NO_x^- concentrations were fit with a function describing the behavior of an oscillating system (22). Baseline fluctuations in NO_x^- concentrations (C_{NOx}) were:

$$dC_{NO_x}/dt = R_{in} - (R_{out} \times C_{NO_x}) \quad (1)$$

$$R_{in} = R_{inm} + (R_{inm} \times A \times \cos(2\pi/\omega \times (t - t_x))) \quad (2)$$

in which R_{in} represents the instantaneous zero-order input rate of NO_x^- into the hippocampus and is dependent on the mean input rate (R_{inm}); A is the amplitude of NO_x^- fluctuations; t_x is the time of peak NO_x^- concentrations (acrophase); ω is the frequency of NO_x^- oscillations; and R_{out} is the first-order rate constant for NO_x^- elimination from the hippocampus. Estimates of R_{inm} and ω were determined by model-independent analysis of the data as shown in Fig. 1 and were held constant during subsequent modeling.

To determine relevant pharmacodynamic parameters for NOS inhibition by 7-NI, a linked pharmacokinetic/pharmacodynamic model was developed. Kinetic parameters obtained from modeling 7-NI disposition and baseline NO_x^- fluctuations were held constant, allowing estimation of the maximal inhibition of NOS (i.e., a decrease in R_{in}) by 7-NI (I_{max}) and the concentration of 7-NI producing 50% maximal inhibition (IC_{50}):

$$dC_{NO_x}/dt = R_{in} \times (1 - I) - (R_{out} \times C_{NO_x}) \quad (3)$$

$$I = (I_{max} \times C_{NO_x})/(IC_{50} + C_{NO_x}) \quad (4)$$

Initial analyses indicated that the model converged with an estimate of I_{max} that exceeded 99%. Because in theory NOS could be inhibited completely by 7-NI, I_{max} was set as a constant (100%), and t_x and IC_{50} were included as parameters in the final model.

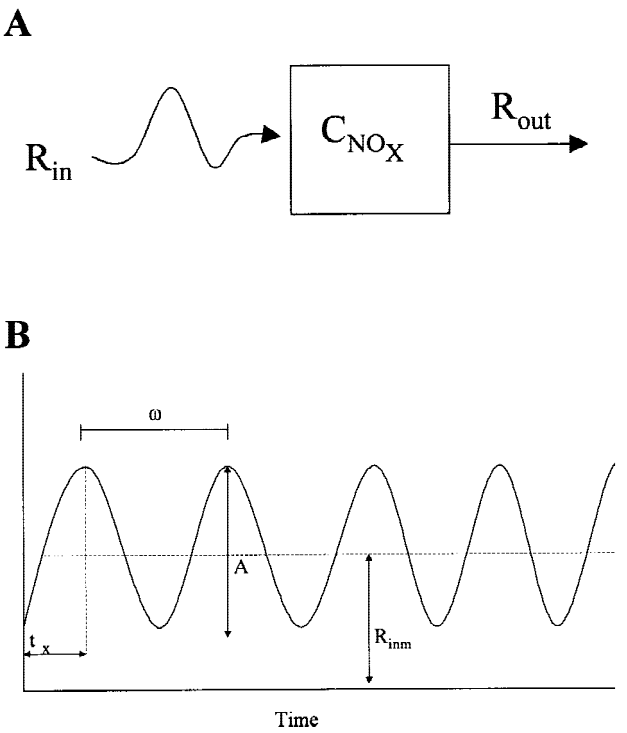

Fig. 1. Scheme for the model describing oscillations of NO_x^- in the hippocampus (A), and a graphical representation of the parameters intrinsic to this model (B). In control animals, R_{in} is simply a function of time; in 7-NI-treated rats, R_{in} is a function of time and 7-NI concentration. Parameter designations are defined in the text.

Model equations were fit to the 7-NI and NO_x^- concentration-time data by nonlinear least-squares regression (WinNonlin, Pharsight Corp., Palo Alto, CA). Assessment of the goodness of fit of the model to the observed data was based on Akaike's Information Criteria, residual plots, coefficients of variation, and confidence intervals of parameter estimates.

RESULTS

7-NI concentration-time profiles in serum and hippocampal extracellular fluid are presented in Fig. 2. *In vivo* microdialysis probe recoveries (mean ± SD) were 25.5 ± 4.8% (range of 19.6–32.3%). Individual probe recoveries were used to correct microdialysate concentrations of 7-NI to provide estimates of 7-NI concentrations in hippocampal extracellular fluid. 7-NI concentrations accumulated gradually in both fluids during repeated administration of 7-NI. A rapid equilibrium between hippocampal and serum 7-NI concentrations was observed; the ratio of 7-NI concentrations in hippocampal extracellular fluid to serum was 0.42 ± 0.02 and did not vary statistically with time (ANOVA, $P > 0.6$). Previous experiments (19) indicated that 7-NI was ~50 to 60% bound in rat serum. When serum concentrations were corrected for protein binding, concentrations of 7-NI in the hippocampus and unbound concentrations in serum were almost identical. The ratio of 7-NI concentrations in hippocampal extracellular fluid to the predicted unbound concentrations in serum (assuming an average $f_u = 0.45$) was 0.92 ± 0.05, indicating that unbound concentrations of 7-NI were essentially equivalent in serum and hippocampal extracellular fluid.

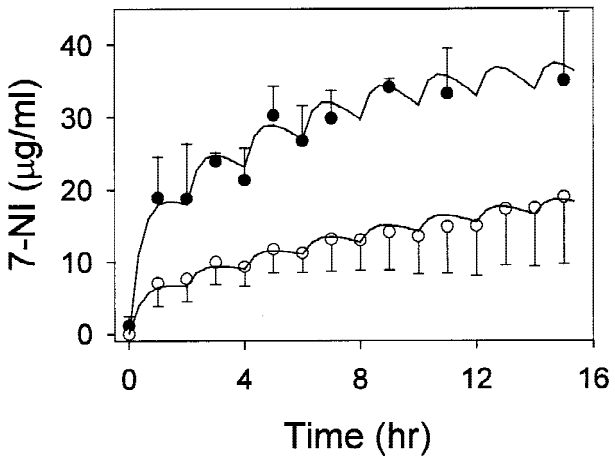

Fig. 2. Concentration-time profiles for 7-NI in serum (●) and hippocampal extracellular fluid (○) after ip administration of a 50-mg/kg loading dose (time 0) plus 25 mg/kg every 2 h. Data are presented as mean ± SD ($n = 4$ per treatment); lines indicate the fit of the pharmacokinetic model to the hippocampal concentration-time data and model predictions of the serum concentration-time profile. Recovered pharmacokinetic parameters were: $k_a = 0.079 \pm 0.010$ h^{-1}; $K = 2.24 \pm 0.94$ h^{-1}; $V_c/F = 4.68 \pm 2.13$ l/kg.

To approximate the disposition of 7-NI in the hippocampus following repeated ip administration, an empirical pharmacokinetic model was fit to the hippocampal extracellular fluid 7-NI concentrations. The correspondence of the model to the observed data is shown in Fig. 2; pharmacokinetic parameter estimates obtained with this model, reported as the estimate and its associated standard error as returned by the regression routine, are presented in the legend to Fig. 2. In general, the model was capable of describing fluctuations in hippocampal 7-NI during the course of the experiment. In addition, by correcting hippocampal concentrations (assumed to be equivalent to unbound serum concentrations) for the presumed degree of protein binding, the model was capable of predicting total 7-NI concentrations in serum (Fig. 2). The parameter estimates, although of limited mechanistic use, were important in constructing the subsequent integrated pharmacokinetic-pharmacodynamic model.

The mean concentration vs. time profile for hippocampal NO_x^- in control rats is presented in Fig. 3. NO_x^- concentrations in the hippocampus displayed cyclic fluctuations (80–120% of baseline) throughout the study, which were observed consistently in individual profiles as well as in the group averages. Pharmacokinetic modeling of these data indicated that NO_x^- fluctuations (amplitude of 0.160 ± 0.043) had a frequency of ~7 h. Acrophase (maximal concentration) occurred at 6.92 ± 0.22 h, coinciding with approximate clock-times of 10 AM, 5 PM, and 12 AM, respectively (relative to a light cycle of 7 AM–7 PM).

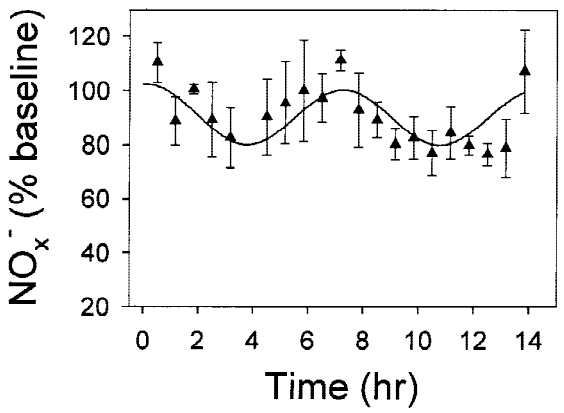

Fig. 3. Fluctuations of hippocampal NO_x^- in control rats. Symbols represent mean ± SD ($n = 4$); line indicates the fit of the kinetic model for oscillating NO_x^- production to the data.

To determine the *in vivo* pharmacodynamic parameters (I_{max} and IC_{50}) associated with inhibition of NOS by 7-NI, a linked pharmacokinetic-pharmacodynamic model was developed. The simultaneous fit of this model to the 7-NI concentrations in hippocampal extracellular fluid and the hippocampal NO_x^- concentration-time data are presented in Figure 4. Associated estimates of pharmacokinetic and pharmacodynamic parameters are presented in the figure legend. Correspondence of the model with the observed data was acceptable, although it should be recognized that the structure of the kinetic portion of the model was empirical. NO_x^- concentrations in the hippocampus decreased during the first 2 h of the experiment (i.e., the pre-7-NI baseline period) due to the cyclic behavior of NO_x^- observed in control animals. Although NO_x^- decreased to only ~85% of the initial concentration in control animals by 4 h, NO_x^- concentrations in 7-NI-treated rats declined to <60% of time 0 concentrations, reaching an initial nadir at ~5.5 h. In both control and 7-NI-treated rats, NO_x^- increased between 5 and 8 h, decreased to a second nadir at ~12 h, with a subsequent increase through the end of the experiment. 7-NI-treated rats displayed, on average, an ~60% decrease in NO_x^- by 12 h. Pharmacodynamic modeling indicated that the *in vivo* IC_{50} for 7-NI in hippocampal extracellular fluid was 17 μg/ml, corresponding to a total serum concentration of ~38 μg/ml, which was achieved by the end of the administration period. Whereas the simple Hill equation was capable of relating changes in NOS activity to 7-NI concentrations in the pharmacokinetic-pharmacodynamic model (Fig. 4), a more complicated relationship was observed between changes in brain tissue NO_x^- and 7-NI concentration (Fig. 5). This relationship was clearly sigmoidal with a maximum increase in NO_x^- concentration of 54%. The 7-NI concentration in hippocampal extracellular

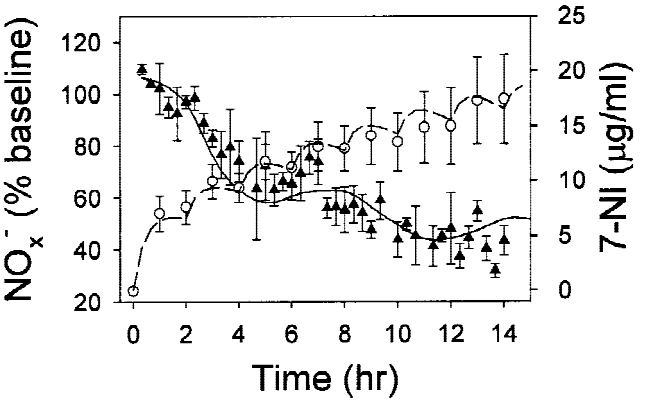

Fig. 4. Fit of the kinetic-dynamic model to NO_x^- (▲) and 7-NI (○) concentrations in hippocampal extracellular fluid. Symbols represent observed data (mean ± SD; $n = 4$ per treatment); lines indicate the model fit. Recovered pharmacodynamic parameters were: $R_{out} = 0.887 \pm 0.019$ h^{-1}; $IC_{50} = 17.2 \pm 1.1$ μg/ml; $I_{max} = 100\%$.

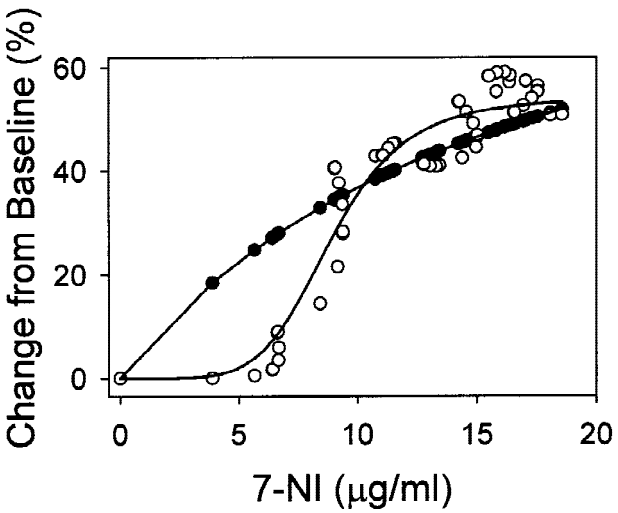

Fig. 5. Comparison of the relationship between effect on hippocampal NO and serum 7-NI for predicted change in NOS activity (●) and observed change in extracellular NO_x^- (○). Symbols represent the mean data as presented in Figure 4 (NO_x^-) or predictions based on the pharmacokinetic-pharmacodynamic model (NOS activity); error bars have been omitted for clarity. Lines represent prediction of the integrated pharmacokinetic-pharmacodynamic model (NOS activity) or empirical fit of the sigmoidal Hill equation to the data (NO_x^- concentrations).

fluid associated with a 27% increase in NO_x^- concentration (i.e., the apparent IC_{50} of 7-NI relative to changes in NOS activity) was ~9 μg/ml.

DISCUSSION

NOS inhibitors have been used extensively as probes to evaluate the physiological roles of NO. However, extensive pharmacokinetic/pharmacodynamic analysis is available only for the non-isoform-selective NOS inhibitor N^{ω}-nitro-L-arginine (16–18). In the absence of reliable macokinetic and macodynamic data, NOS inhibitors must be administered empirically, limiting the reliability with which differing study designs can be compared. Previous experiments (19) were performed to evaluate the pharmacokinetics of 7-NI when administered as a single ip dose. These data indicated that 7-NI disposition was nonlinear over the dose range of 10 to 50 mg/kg, which could complicate the design of experiments directed toward providing a specific degree of NOS inhibition. The present study was performed to evaluate the disposition of 7-NI in the rat hippocampus during continuous administration of 7-NI and to evaluate the pharmacodynamics of 7-NI-mediated inhibition of NOS.

Comparison of 7-NI concentrations in serum and hippocampus (Fig. 2) indicated that 7-NI distributed rapidly into the brain from the systemic circulation. In addition, when serum concentrations of 7-NI were corrected for estimates of protein binding, unbound concentrations in the serum and concentrations in hippocampal extracellular fluid were almost identical. These observations suggest that 7-NI distributes passively across the blood-brain barrier. Therefore, serum concentrations of 7-NI, corrected for a known extent of protein binding, can be used as a surrogate for unbound 7-NI concentrations in the CNS. The present data allow the design of administration regimens that can maintain specified 7-NI concentration ranges in the brain.

To evaluate the relationship between 7-NI concentrations and inhibition of NOS in the hippocampus, the pharmacodynamics of 7-NI-mediated inhibition of brain NOS was examined with *in vivo* microdialysis. Due to the extremely short *in vivo* half-life of NO, the Griess assay for NO_x^- was used as an indirect measure of NO concentrations. Experiments in control rats indicated that NO_x^- concentrations displayed cyclic fluctuations throughout a 14-h period (Fig. 3). Although the mechanism for these fluctuations is unknown, previous studies (23) indicated that L-arginine concentrations in the CNS display time-dependent fluctuation with higher concentrations in the morning and decreased concentrations in the evening. Because L-arginine is the precursor of NO, such fluctuations may be responsible for the observed cycling of NO_x^-. In addition, the effects of 7-NI on electroencephalographic power spectra in rats were more prominent during the day than during the night (24), consistent with higher NO concentrations (and therefore an enhanced potential for inhibition) during the day. These authors concluded that NO exerts an excitatory circadian effect on the neuronal structures responsible for the control of vigilance. Circadian changes in NOS activity also have been observed (25). These reports all suggest that the rate of NO production is a light-cycle-dependent circadian process dependent on changes in the available precursor and/or the activity of the enzyme. The present results also indicate a cyclic pattern of NO production; however, the frequency of the observed oscillations (~7 h) is not typical of a circadian process (~24 h). Due to the intensive dosing and sampling schedule in the present experiment, the normal light cycle was interrupted (due to activating room lights to obtain samples), possibly resulting in a perturbation of the physiological circadian rhythm.

Administration of 7-NI resulted in significant inhibition of NOS activity in the rat hippocampus (Fig. 4). The magnitude of inhibition of NOS appeared to be correlated with hippocampal concentrations of 7-NI. It was not feasible to develop a simple, static relationship between changes in NO_x^- and 7-NI concentrations due to the cyclic pattern of NO_x^- in control animals. Thus, despite the fact that the relevant site of action was pharmacokinetically indistinguishable from the central compartment, it was necessary to resort to pharmacokinetic/pharmacodynamic modeling to evaluate the relationship between 7-NI exposure and NO_x^- in the hippocampus.

Multiple-dose administration of 7-NI was capable of inhibiting NOS activity in the brain for an extended period. The results of this study serve as an aid in the design of future experiments involving 7-NI and would allow design of dosing regimens to attain specific degree of NOS inhibition for selected periods of time. Parameters describing the inhibition of NOS by 7-NI have been reported in the literature previously. Wolff and Gribbin (8) reported that inhibition of NOS by 7-NI exhibits a K_i of 0.16 μM for neuronal NOS as compared with 1.6 μM for the inducible isoform of NOS. In contrast, the *in vivo* IC_{50} is ~100 μM as documented in the present series of experiments. Whereas *in vitro* data provide important information regarding selectivity and mechanisms of inhibition relative to other NOS inhibitors, their use in predicting the *in vivo* concentrations necessary to attain a desired level of NOS inhibition is limited.

In summary, the present study provides an extensive evaluation of the pharmacokinetics and *in vivo* pharmacodynamics of 7-NI. These experiments indicated that 7-NI rapidly

equilibrates with the CNS most likely by passive diffusion. As a result, total serum concentrations corrected for protein binding provided a reliable estimate of 7-NI concentrations in hippocampal extracellular fluid. Pharmacokinetic/pharmacodynamic modeling indicated that 7-NI was capable of inhibiting NOS activity with an apparent IC_{50} of ~17 μg/ml. These data serve as an aid for the development of rational 7-NI dosing regimens that will provide a desired magnitude of NOS inhibition.

REFERENCES

1. C. C. Huang and K. S. Hsu. Nitric oxide signaling is required for the generation of anoxia-induced long-term potentiation in the hippocampus. *Eur. J. Neurosci*. **9**:2202–2206 (1997).
2. L. J. Herberg, A. Grottick, and I. C. Rose. Nitric oxide synthesis, epileptic seizures and kindling. *Psychopharmacology* **119**:115–123 (1995).
3. M. Qiang, Y. C. Chen, R. Wang, F. M. Wu, and J. T. Qiao. Nitric oxide is involved in the formation of learning and memory in rats: studies using passive avoidance response and Morris water maze task. *Behav. Pharmacol*. **8**:183–187 (1997).
4. I. D. G. Duarte, B. B. Lorenzetti, and S. H. Ferreira. Peripheral analgesia and activation of the nitric oxide-cyclic GMP pathway. *Eur. J. Pharmacol*. **186**:289–293 (1990).
5. J. Y. Xu, K. P. Hill, and J. M. Bidlack. The nitric oxide/cyclic GMP system at the supraspinal site is involved in the development of acute morphine antinociceptive tolerance. *J. Pharmacol. Exp. Ther*. **284**:196–201 (1998).
6. I. T. Uzbay, B. F. Erden, E. E. Tapanyigit, and S. O. Kayaalp. Nitric oxide synthase inhibition attenuates signs of ethanol withdrawal in rats. *Life Sci*. **61**:2197–2209 (1997).
7. P. K. Moore and R. L. Handy. Selective inhibitors of neuronal nitric oxide synthase–is no NOS really good NOS for the nervous system? *TIPS* **18**:204–211 (1997).
8. D. J. Wolff and B. J. Gribbin. The inhibition of the constitutive and inducible nitric oxide synthase isoforms by indazole agents. *Arch. Biochem. Biophys*. **311**:300–306 (1994).
9. B. T. Callahan and G. A. Ricaurte. Effect of 7-nitroindazole on body temperature and methamphetamine-induced dopamine toxicity. *NeuroReport* **9**:2691–2695 (1998).
10. K. Ikeda, Y. Iwasaki, and M. Kinoshita. Neuronal nitric oxide synthase inhibitor, 7-nitroindazole, delays motor dysfunction and spinal motoneuron degeneration in the wobbler mouse. *J. Neurol. Sci*. **160**:9–15 (1998).
11. S. F. Ali and Y. Itzhak. Effects of 7-nitroindazole, an NOS inhibitor on methamphetamine-induced dopaminergic and serotonergic neurotoxicity in mice. *Ann. NY Acad. Sci*. **844**:122–130 (1998).
12. M. Takahashi, R. Izumi, and H. Kaneto. Comparative studies on morphine- and stress-induced analgesia and the development of tolerance to the effects: implication of protein synthesis mechanism in the process. *Jpn. J. Pharmacol*. **37**:197–202 (1985).
13. N. Zamir and M. Segal. Hypertension-induced analgesia: changes in pain sensitivity in experimental hypertensive rats. *Brain Res*. **160**:170–173 (1979).
14. R. C. Meyer, E. L. Spangler, N. Patel, E. D. London, and D. K. Ingram. Impaired learning in rats in a 14-unit T-maze by 7-nitroindazole, a neuronal nitric oxide synthase inhibitor, is attenuated by the nitric oxide donor, molsidomine. *Eur. J. Pharmacol*. **341**: 17–22 (1998).
15. K. J. Escott, J. S. Beech, K. K. Haga, S. C. Williams, B. S. Meldrum, and P. M. Bath. Cerebroprotective effect of the nitric oxide synthase inhibitors, 1-(2-trifluoromethylphenyl) imidazole and 7-nitro indazole, after transient focal cerebral ischemia in the rat. *J. Cerebr. Blood Flow Metab*. **18**:281–287 (1998).
16. M. A. Tabrizi-Fard and H. L. Fung. Pharmacokinetics, plasma protein binding and urinary excretion of N-nitro-L-arginine in rats. *Br. J. Pharmacol*. **111**:394–396 (1994).
17. M. A. Tabrizi-Fard and H. L. Fung. Pharmacokinetics and steady-state tissue distribution of L- and D- isomers of nitroarginine in rats. *Drug Metab. Dispos*. **24**:1241–1246 (1996).
18. M. A. Tabrizi-Fard and H. L. Fung. Effects of nitro-L-arginine on blood pressure and cardiac index in anesthetized rats: a pharmacokinetic-pharmacodynamic analysis. *Pharm. Res*. **15**:1063–1068 (1998).
19. M. A. Bush and G. M. Pollack. Pharmacokinetics and protein binding of the selective neuronal nitric oxide synthase inhibitor 7-nitroindazole. *Biopharm. Drug Dispos*. **21**:221–228 (2000).
20. A.-K. Colin. *Microdialysis User's Guide, 4th edition*. Carnegie Medicin, Stockholm, Sweden, 1988.
21. M. Feelisch and J. S. Stamler. *Methods in Nitric Oxide Research*. John Wiley & Sons, New York, 1996.
22. K. H. Lew, E. A. Ludwig, M. A. Milad, K. Donovan, E. Middleton, J. J. Ferry, and W. J. Jusko. Gender-based effects on methylprednisolone pharmacokinetics and pharmacodynamics. *Clin. Pharmacol. Ther*. **54**:402–414 (1993).
23. I. Buchmann, L. Milakofsky, N. Harris, J. M. Hofford, and W. H. Vogel. Effect of arginine administration on plasma and brain levels of arginine and various related amino compounds in the rat. *Pharmacology* **53**:133–142 (1996).
24. E. Dzoljic, R. van Leeuwen, R. de Vriew, and M. R. Dzoljic. Vigilance and EEG power in rats: effects of potent inhibitors of the neuronal nitric oxide synthase. *N.-S. Arch. Pharmacol.* **356**: 56–61 (1997).
25. N. A. Ayers, L. Kapas, and J. M. Krueger. Circadian variation of nitric oxide synthase activity and cytosolic protein levels in rat brain. *Brain Res*. **707**:127–130 (1996).